

Ultraviolet Absorption of Insulators. II. Partially Ionic Crystals*

J. C. PHILLIPS†

Department of Physics, University of Chicago, Chicago, Illinois

(Received 27 May 1963; revised manuscript received 6 September 1963)

A wide range of experimental data now indicates that uv structure depends primarily on crystal structure and only secondarily on atomic composition. We assign characteristic structure of ultraviolet absorption to interband transitions at symmetry points of the Brillouin zone. The crystal structures that are discussed are zincblende and wurtzite. The experimental information required for comparison with theoretical calculations is discussed, with special emphasis laid on the importance of polarization studies of the reflectance of hexagonal crystals.

1. INTRODUCTION

THE electronic states of insulators may be classified into two broad categories: the infrared states within 1 eV of the valence band maximum or the conduction band minimum; and the uv states between 1 and 10 eV away from those edges. For E more than 10 eV below the valence band edge, one deals with core states similar to those of the free atom (more generally, free ion). For E more than 10 eV above the conduction band edge, the spectrum of an insulator looks similar to that of a metal or a free-electron gas.

Until quite recently, almost all experimental studies of the electronic structure of insulators were confined to the infrared states. From the theorists' viewpoint this was most unsatisfactory. Band calculations give all the electronic states within 10 eV of the energy gap. Only a few of these fall in the infrared category. If one or two of these should be given incorrectly by theory, the band calculations are made to appear entirely unreliable. The picture is much more balanced when experimental data on the ultraviolet category are available as well.

Considering the conceptual importance of the uv region and the vast effort that has been expended on the infrared region, one may well ask why it is only recently that attention has focused on the ultraviolet. The obstacle was primarily one of interpretation. Interband structure has been known¹ in the far-uv spectra of alkali halides for more than three decades. The structure apparently consisted of broad ($\Delta E \sim 0.5$ eV) peaks spaced at irregular intervals of 1 or 2 eV. As no theoretical interpretation of this structure was forthcoming, attention was focussed on the sharp ($\Delta E \lesssim 0.1$ eV) exciton peaks which conformed to a trival hydrogenic spectrum. We will see later that lack of proper theoretical guides has obscured the intrinsic structure in much of the data. In the absence of this structure, it is not surprising that theorists have paid little attention to the ultraviolet.

The first step away from this impasse was taken by Philipp and Taft, who examined the uv spectra of crystals whose infrared spectra were well understood.

They made extremely careful measurements of the reflectance from etched crystals of Ge (Ref. 2) and Si (Ref. 3) over the energy range 1–10 eV. By using the Kramers–Kronig relations they derived ϵ_1 and ϵ_2 , the real and imaginary parts of the dielectric constant, respectively, over this range. Neglecting lifetime broadening, the contribution of direct transitions to ϵ_2 is

$$\epsilon_2(\omega) = \frac{e^2 \hbar^2}{m} \sum_{i,j} \frac{1}{\Omega} \int_{\text{BZ}} \frac{f_{ij}(\mathbf{k})}{(E_j - E_i)} \delta(E_i - E_j - \hbar\omega) d\mathbf{k}, \quad (1.1)$$

where i and j are valence and conduction band states, respectively. Here Ω is the volume of the Brillouin zone. The interband oscillator strength f_{ij} is defined by⁴

$$f_{ij}(\mathbf{k}) = \frac{2}{3m} \frac{|\langle \mathbf{k}_j | \hat{p} | \mathbf{k}_i \rangle|^2}{E_j - E_i}. \quad (1.2)$$

The next step⁵ was to realize that if $f_{ij}(\mathbf{k})$ varies smoothly with \mathbf{k} (as it must, according to perturbation theory), then the characteristic structure of ϵ comes from the δ function in (1.1). To see this, transform (1.1) to an integral over a surface of constant energy

$$\epsilon_2(\omega) = \frac{e^2 \hbar^2}{m} \sum_{i,j} \frac{1}{\Omega} \int \frac{f_{ij}(\mathbf{k})}{E_{ij} |\nabla_k E_{ij}|} dS_k, \quad (1.3)$$

where $E_{ij}(\mathbf{k}) = E_j(\mathbf{k}) - E_i(\mathbf{k})$. The density of states having the energy difference E_{ij} is proportional.

$$\frac{dN_{ij}}{dE} \sim \int \frac{1}{|\nabla_k E_{ij}|} dS_k. \quad (1.4)$$

By comparing (1.3) and (1.4) we see that the analytic singularities in dN_{ij}/dE are reproduced in $\epsilon_2(\omega)$ with a neglecting factor proportional to f_{ij}/E_{ij} . A general theory of analytic singularities in dN_{ij}/dE due to $|\nabla_k E_{ij}| = 0$ has been developed.^{6,7} The points in k space where $\nabla_k E_{ij} = 0$ are called critical points. The cor-

² H. R. Philipp and E. A. Taft, Phys. Rev. **113**, 1002 (1959).

³ H. R. Philipp and E. A. Taft, Phys. Rev. **120**, 37 (1960).

⁴ F. Seitz, *The Modern Theory of Solids* (McGraw-Hill Book Company, Inc., New York, 1940).

⁵ J. C. Phillips, J. Phys. Chem. Solids **12**, 208 (1960).

⁶ L. Van Hove, Phys. Rev. **89**, 1189 (1953).

⁷ J. C. Phillips, Phys. Rev. **104**, 1263 (1956).

* Supported in part by the National Science Foundation.

† Guggenheim Fellow with a grant-in-aid from the Sloan Foundation.

¹ R. Hilsch and R. W. Pohl, Z. Physik **59**, 812 (1930).

responding singularities in dN_{ij}/dE or ϵ_2 will be called Van Hove singularities here.

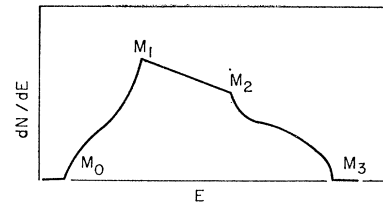
The principal singularities in the uv spectrum of Ge were tentatively (and essentially correctly) identified⁵ as Van Hove singularities due to critical points at $\mathbf{k}=\mathbf{L}=\pi a^{-1}(111)$ and $\mathbf{X}=\pi a^{-1}(200)$. Nevertheless, the identification of the latter critical point was quite uncertain. The reason for this uncertainty is that there must be⁷ a large number of Van Hove singularities in (1.1). The singularities are of various kinds, as shown in Fig. 1. If $E_{ij}(\mathbf{k})$ has a relative minimum at E_0 , we obtain a singularity M_0 corresponding to the usual threshold familiar from the direct infrared absorption edge. Ultraviolet M_0 's turn out to be weak and difficult to identify. The peaks in the structure are in fact absorption edges associated with saddle points M_1 and M_2 of the first and second kinds, respectively. In order to explain the strongest peak in ϵ_2 for Ge it was necessary to postulate⁵ two singularities, an M_1 at 4.5 eV and an M_2 at 4.6 eV. That two singularities should be so nearly degenerate seemed a remarkable accident. It also posed a major theoretical problem, in so far as energy-band calculations for Si and Ge had frequently made errors of several eV. The accuracy required to reproduce $\epsilon_2(\omega)$ appeared to be beyond the limitations imposed by uncertainties in the crystal potential.⁸

Two ways out of this dilemma were found. The first⁹ was an analysis of ultraviolet spectra of a wider range of mostly covalent crystals, including a number of 3-5 crystals like GaAs. One of the most important clues in this semiempirical analysis was provided by a nominally infrared experiment, cyclotron resonance. The effective masses measured by this experiment are of the form (e.g., for band i isotropic)

$$m/m_i^* = 1 - 3\sum_j f_{ij}. \quad (1.5)$$

Here f_{ij} is given by (1.2). The matrix elements p_{ij} can be determined quite accurately by theory. (They are also found to be nearly constant for a given crystal structure over a wide range of atomic compositions.) Ever since the initial cyclotron resonance experiments¹⁰ an important ambiguity had remained about one of the effective mass parameters for the top of the valence band of Si at $\mathbf{k}=\mathbf{\Gamma}=0$. This parameter emerged as a root of a quadratic equation. According to one choice of sign¹⁰ a level $j=\Gamma_2'$ was 9 eV higher in Si than in Ge. The other choice¹¹ made it 3 eV higher. Theory showed¹² that Γ_2' was twice as sensitive as L_1 to changes in atomic composition. As discussed in I, this conclusion was con-

FIG. 1. Van Hove singularities in the density of states of $E(\mathbf{k})$ ranging over a three-dimensional Brillouin zone.



firmed by the effect of pressure and alloying. Measurement of the sign (carried out most cleverly by cyclotron resonance in a strained sample¹³) gave $\delta E_{ij}=3$ eV. Nearly all other levels at the principal symmetry points \mathbf{k}_α ($\alpha=\Gamma, L, X$) were thought to be ten times relatively less sensitive to changes in atomic composition. This conclusion was confirmed by the uv spectra, which showed in particular that the separation of the M_1 and M_2 singularities responsible for the largest peak did not vary by more than 0.2 eV for ten different atomic compositions of the same crystal structure (diamond or zincblende).

With these conclusions in hand it was possible to make a categorical classification⁹ of the energy levels at the principal symmetry points \mathbf{k}_α . Here the most important critical points should occur because $\nabla_{\mathbf{k}}E=0$ by symmetry. The same classification predicted that more careful measurements of certain peaks in the vacuum ultraviolet (beyond 5 eV) would reveal spin-orbit splittings. Now that a theoretical interpretation was available, progress was made rapidly. First the predicted spin-orbit splitting was observed.¹⁴ A number of experimental papers now appeared, with sufficiently high resolution to detect Van Hove singularities that had been previously overlooked.

The second theoretical task was to determine the line shape by an accurate evaluation of (1.1), not just at the symmetry points \mathbf{k}_α , but by sampling $E(\mathbf{k})$ throughout the Brillouin zone. Because the levels at the symmetry points \mathbf{k}_α were known (again tentatively, of course), all that was required was a scheme that would interpolate to an accuracy better than 0.1 eV. The insensitivity of the spectrum to changes in atomic composition strongly suggested that a scheme based on the shape of the Brillouin zone alone (i.e., a nearly free-electron scheme) would suffice. The pseudopotential method¹¹ was designed for just this purpose. In view of the cancellation theorem¹⁵ the pseudopotential was expected to be insensitive to changes in atomic cores, as required. The cancellation theorem implies $V_{\mathbf{K}}$ (the \mathbf{K} th Fourier transform of the pseudopotential, \mathbf{K} being a reciprocal lattice vector) is zero after the first two or three reciprocal lattice vectors. It had already been demonstrated¹⁶ that this gave excellent convergence and smooth $E(\mathbf{k})$ curves in the infrared region.

⁸ J. C. Phillips and L. Kleinman, Phys. Rev. **128**, 2098 (1962).

⁹ J. C. Phillips, Phys. Rev. **125**, 1931 (1962), hereafter referred to as I.

¹⁰ G. F. Dresselhaus, A. F. Kip, and C. Kittel, Phys. Rev. **98**, 368 (1955).

¹¹ J. C. Phillips, Phys. Rev. **112**, 685 (1958).

¹² F. Herman and S. Skillman, in *Proceedings of the International Conference on Semiconductor Physics, 1960* (Czechoslovakian Academy of Sciences, Prague, 1961, and Academic Press Inc., New York, 1961).

¹³ J. C. Hensel and G. Feher, Phys. Rev. **129**, 1041 (1963).

¹⁴ H. Ehrenreich, H. R. Philipp, and J. C. Phillips, Phys. Rev. Letters **8**, 59 (1962).

¹⁵ M. H. Cohen and V. Heine, Phys. Rev. **122**, 1821 (1961).

¹⁶ F. Bassani and V. Celli, J. Phys. Chem. Solids **20**, 64 (1961).

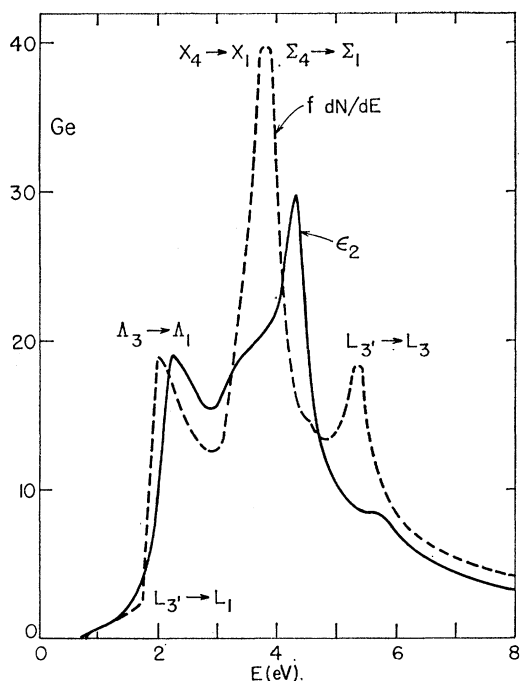


FIG. 2. The experimental values of $\epsilon_2(\omega)$ in Ge compared to the theoretical value calculated from Eq. (1.3) by the pseudopotential method.

With these considerations in mind a pseudopotential chosen to fit infrared levels in Ge was used to solve the necessary 90×90 secular equations at more than 1000 points distributed regularly through the basic volume filling $1/48$ th of the Brillouin zone. The results¹⁷ were astonishing (see Figs. 2 and 3). Not only was the gross structure of ϵ_2 reproduced; the exact separation of many pairs of Van Hove singularities was given to 0.05 eV, which has turned out¹⁸ to be the convergence limit of accuracy of the interpolation. A similar calculation¹⁹ for Si (see Figs. 4 and 5) gave excellent agreement with experiment for $\epsilon_2(\omega)$. It also gave a remarkably detailed picture of photoelectric yield and energy distribution which is in excellent agreement with experiment.^{20,21}

With the theoretical line shape in hand it now became possible to resolve M_0 thresholds in the uv—sometimes even spin-orbit split thresholds.²² The systematics of interpretation now appear to be solved, at least for the zincblende and diamond structures.²³

To enable the reader to appreciate the impact of uv spectra on our knowledge of the electronic structure of insulators, a survey of information collected by “in-

¹⁷ D. Brust, J. C. Phillips, and F. Bassani, Phys. Rev. Letters **9**, 94 (1962).

¹⁸ D. Brust (to be published).

¹⁹ D. Brust, M. L. Cohen, and J. C. Phillips, Phys. Rev. Letters **9**, 389 (1962).

²⁰ F. G. Allen and G. W. Gobeli, Phys. Rev. **127**, 141 (1962).

²¹ W. E. Spicer and R. E. Simon, Phys. Rev. Letters **9**, 385 (1962).

²² D. L. Greenaway, Phys. Rev. Letters **9**, 97 (1962).

²³ M. Cardona and D. L. Greenaway, Phys. Rev. **131**, 98 (1963).

TABLE I. “Infrared” energy differences between conduction and valence band states in semiconductors with diamond or zincblende crystal structure. Some energy differences can be roughly inferred from theoretical interband matrix elements and effective masses measured by cyclotron resonance; these are underlined.

Direct edges	$\Gamma_{25'}^{3/2} - \Gamma_{2'}$	$\Gamma_{25'}^{1/2} - \Gamma_{25'}^{3/2}$
Ge	0.8	0.3
Si	0.7	0.05
GaAs	1.35	0.3
GaSb	0.7	
InAs	0.3	
InSb	0.2	
InP	1.3	
ZnTe	2.3	
CdTe	1.6	
HgTe	0.02	
HgSe	0.6	
ZnSe	2.7	
AlSb	1.6	
Sn	0.1	

Indirect edges and cyclotron resonance					
	L_1	X_1	L_3'	X_4	Γ_{15}
Ge					
Ge	0.7	0.9	2		
Si		1.1		4	3
GaP		2.2			
C		5.4			

frared” experiments on about 20 crystals having diamond or zincblende crystal structures is made in Table I. These data, collected by many workers over a period of more than 10 years, give the position of 24 energy differences between valence and conduction band states.

It is interesting to contrast Table I with Table II, which lists the “ultraviolet” energy differences collected by only a few experimentalists (chiefly Philipp and Cardona) during the last 4 years. Although there are obviously many gaps in Table II, it already contains 107 entries. These demonstrate conclusively that ultraviolet spectra, backed by proper theoretical analysis, represent *the* way to study the electronic structure of insulators.

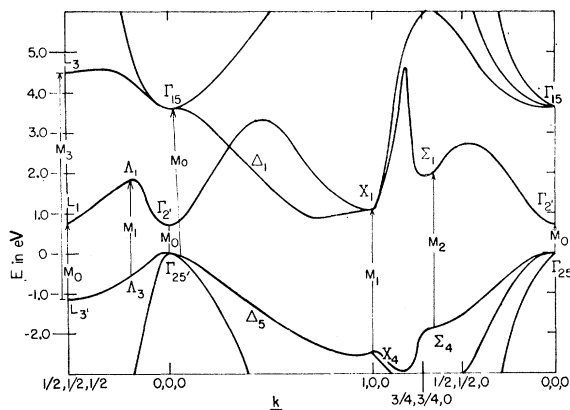


FIG. 3. The energy bands of Ge according to the pseudopotential method. The interband critical points responsible for many of the Van Hove singularities in Fig. 2 are labeled.

TABLE II. "Ultraviolet" energy differences between conduction and valence band states in semiconductors with diamond or zincblende crystal structure. As the latter can be considered a slightly perturbed version of the former, it is permissible to use the diamond symmetry designations of all levels. Several zincblende transitions of the type $X_5 \rightarrow X_3$ (see Ref. 22) have been omitted from this table. As in Table I, we do not give the many references for all the data, as the table is intended only to be schematic. Most of the necessary references are mentioned in the text. The C data are taken from W. C. Walker and J. Osantowski (to be published).

	$(L_3'L_1)$	$(\Lambda_3\Delta_1)$	$(\Gamma_{25'}\Gamma_{15})$	(X_4X_1)	$(L_3'L_3)$	$(L_3'L_2')$
Ge	2.0, 2.2	2.2, 2.4	3.2	4.3	5.7	
Si	3.2		3.7	4.4	5.5	
InSb		1.8, 2.3	2.8, 3.5	4.1	5.3, 6.0	
InAs	2.4	2.5, 2.8	3.9	4.7	6.4, 7.0	
GaSb	1.2, 1.7	2.0, 2.5	3.7	4.3		
GaAs	2.5, 2.7	3.0, 3.2	4.2, 4.5	5.1	6.6, 6.9	
InP		3.1, 3.3		5.0		
AlSb		2.8				
GaP		3.7	3.7	5.3		
HgTe	2.0, 2.7	2.2, 2.9	4.1	4.9, 5.1	6.5, 7.8	9.7
CdTe	3.7	3.4, 4.0	5.2	5.5, 5.7	6.8, 7.6	10.1
ZnTe	3.5, 4.0	3.6, 4.1	4.8	5.4	6.9, 7.5	10.6
HgSe		2.8, 3.1				
ZnSe		4.9, 5.3			9.1, 9.6	
C	16.7		7.3	12.6		
Sn		1.3, 1.7		3.6		
CuCl		6.5	6.8	8.3		
CuBr		5.5, 5.6	6.6	7.3		
CuI		4.8, 5.1	6.0, 6.4	7.3, 7.9		
AgI		5.0, 5.4	6.8, 7.7	8.7		

In spite of the vast progress that has occurred so rapidly, there are still interesting problems connected with the uv spectra of zincblende and wurtzite structures. Cardona^{23,24} has emphasized that the empirical regularities of the diamond and zincblende spectra should carry over to wurtzite, even though the latter crystal structure is hexagonal rather than cubic.

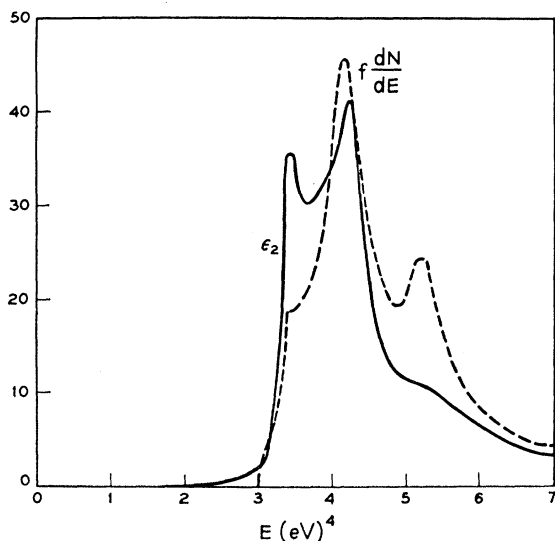


FIG. 4. The experimental values of $\epsilon_2(\omega)$ in Si compared to the theoretical value calculated from Eq. (1.3) by the pseudopotential method.

²⁴ M. Cardona, Phys. Rev. **129**, 1068 (1963).

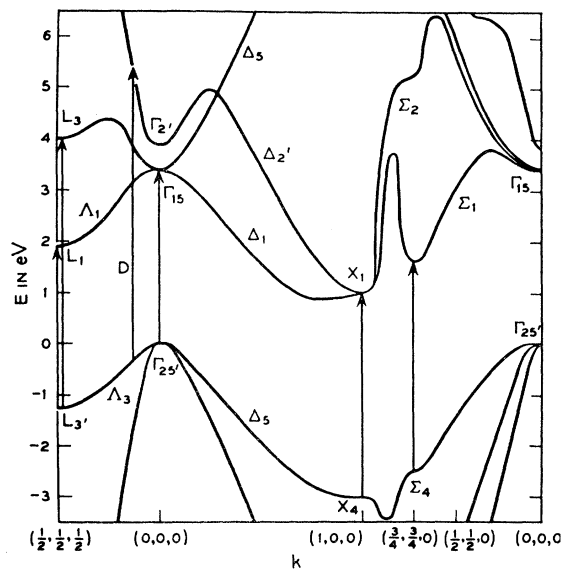


FIG. 5. The energy bands of Si according to the pseudopotential method. Again the important critical points are marked.

With these questions in mind we take up some few unresolved points about zincblende spectra in Sec. 2. In Sec. 3 we take advantage of the close similarity between the spectra of crystals in the zincblende and wurzite modifications to discuss the energy levels at symmetry points of the hexagonal zone. Although our discussion is restricted to symmetry points (and therefore can say nothing about line shape), the rapid development of this field appears to warrant a theoretical review similar to that of I. We find that with the aid of recent polarization data²⁵ (stimulated in part by a preliminary version of this paper), it is possible to guess a great deal about the band structure of wurzite, which has hitherto proved almost intractable.

2. ZINCBLLENDE SPECTRA

The zincblende crystal structure is the same as that of diamond, except that the two atoms in the unit cell are different. We divide the crystal potential into parts symmetric and antisymmetric with respect to inversion about an origin midway between the two atoms in the unit cell. The band structure derived from the symmetric potential can be determined from the known band structures of Si, Ge, and grey Sn. The antisymmetric or polar potential can be treated as a perturbation which introduces a matrix element between bonding valence band states and antibonding conduction band states.²⁶ By solving the two-by-two secular equation, one obtains an expression for zincblende spectra corresponding to the transitions $\Gamma_{25'} \rightarrow \Gamma_{15}$, $X_4 \rightarrow X_1$, $L_3' \rightarrow L_3$, and $L_3' \rightarrow L_1$ of diamond-type crystals. If the polar potential is taken to be proportional to λ ($\lambda = 1$ for 3-5 crystals, 2 for 2-6,

²⁵ M. Cardona, Solid State Communications **1**, 109 (1963).

²⁶ F. Herman, J. Electronics **1**, 103 (1955).

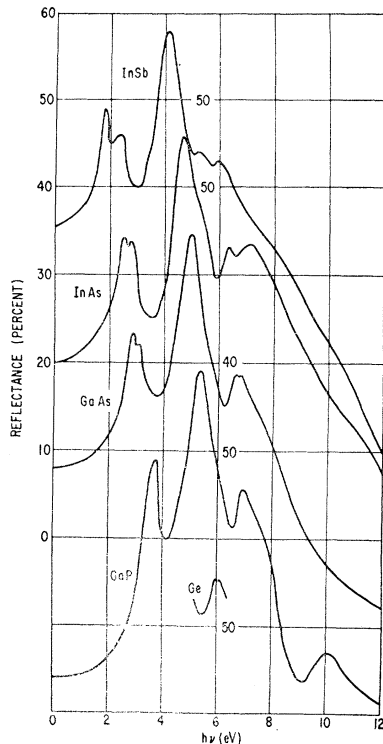


FIG. 6. The ultraviolet reflectance of several 3-5 zincblende crystals. Note the abnormal peak in the reflectance of GaP near 10 eV.

and 3 for 1-7) an excellent fit to experiment is found.²³

The last interband structure in Ge is the $L_{3'} \rightarrow L_3$ transition which gives a weak peak between 5.6 and 5.7 eV. In the zincblende crystals, further structure is observed above 6 eV. This is not surprising, for if we compare Ge, say, with GaAs below 6 eV, we notice that the polar potential not only increases the separation of valence and conduction bands; it also tends to sharpen the spectral structure. This is because the polar potential tends to flatten $E(k)$ in both valence and conduction bands, in accordance with the tendency of ionic crystals to more nearly tight-binding than free-electron (compare, e.g., diamond and cubic BN²⁷).

The uv reflectance of several 3-5 zincblende crystals is shown¹⁴ in Fig. 6. Between 8 and 12 eV there are faint (but genuine) oscillations in the reflectance which are due to Van Hove singularities in ϵ_2 . Unfortunately, the oscillations are so weak that it is not possible at present to identify corresponding oscillations in the theoretical histograms for Ge¹⁷ or Si.¹⁹ The limits of accuracy¹⁸ of these calculations do not offer much hope that addition of a weak polar potential would resolve the oscillations.

In the GaP spectrum, on the other hand, there is a large peak near 10 eV. It appears that this peak is caused by an M_0 singularity at 9.3 eV, an M_1 singularity at 9.8 eV, and possibly an M_2 singularity at 10.4 eV.

The strength of this peak is somewhat surprising, because, at 10 eV, most of the valence band \rightarrow conduction band oscillator strength has been exhausted (f -sum rule). Just this point gives us confidence to identify the

singularities responsible for the peak. It has been suggested¹⁴ that at least one of these singularities may come from the transition $\Gamma_{25'} \rightarrow \Gamma_{12'}$. Here $\Gamma_{12'}$ is the lowest lying state of entirely d atomic symmetry. (In Ge it corresponds to bonding $4d$ orbitals.) There is no other experimental evidence for the position of $\Gamma_{12'}$, but theory indicates¹¹ $E(\Gamma_{12'}) - E(\Gamma_{25'}) \sim 9$ or 10 eV. We note that s states are much more sensitive to changes in atomic composition than p states,^{9,12} so that $E(\Gamma_{12'})$ may be even less sensitive to shortcomings of our calculations than $E(\Gamma_{25'})$. Finally, $|\langle \Gamma_{12'} | p | \Gamma_{25'} \rangle|^2$ is about 0.3 $|\langle \Gamma_{15} | p | \Gamma_{25'} \rangle|^2$ so that the oscillator strength associated with this transition ($4p \rightarrow 4d$, both bonding, in Ge) is appreciable.²⁷

If we now examine other transitions at Γ , X , and L , the ones with appreciable oscillator strength should occur between levels which are almost degenerate in the nearly free-electron approximation. This suggests ($L_{3'}L_{2'}$) which theory indicates²⁸ differ by about 10 eV. In the diamond structure dipole transitions between these states are forbidden by group theory, but in the neighborhood of L , the oscillator strength is comparable to that of $\Gamma_{25'} \rightarrow \Gamma_{12'}$. In the zincblende structure, dipole transitions are allowed in proportion to the strength λ of the polar potential.

We suggest²⁹ that the large peak near 10 eV in GaP is due to transitions in the general neighborhood of $L_{3'} \rightarrow L_{2'}$. Because an exhaustive study of the band $4 \rightarrow$ band 8 interband density of states has not been made, it is not possible at present to specify the positions of the singularities more precisely. Note that the oscillator strength of $\Gamma_{25'} \rightarrow \Gamma_{12'}$ transitions is little changed on going from GaP to Si or Ge, yet no peak is observed in the absence of the polar potential. If our

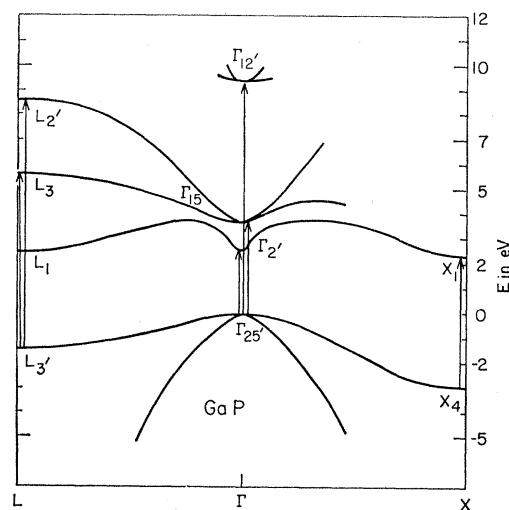


FIG. 7. The energy bands of GaP as inferred from uv interband transitions.

²⁷ L. Kleinman and J. C. Phillips, Phys. Rev. 117, 460 (1960).

²⁸ L. Kleinman and J. C. Phillips, Phys. Rev. 118, 1153 (1960).

²⁹ D. Brust (private communication).

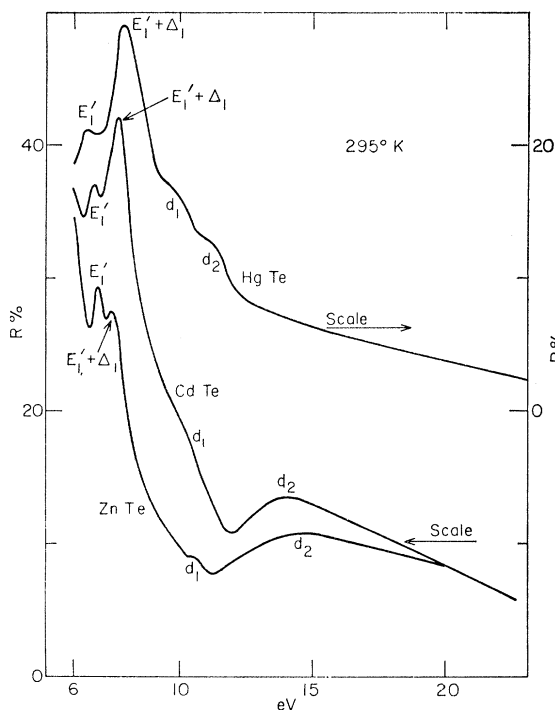


FIG. 8. The uv reflectance of Zn, Cd, and HgTe. Note the structure labeled d_1 and d_2 .

qualitative assignments are correct, the energy bands of GaP will look as shown in Fig. 7. The 10-eV peak in GaP is classified as an (L_3, L_2') peak in Table II.

We now turn to the 2-6 zincblende spectra shown²⁸ in Fig. 8. Above 9 eV, ZnTe, CdTe, and HgTe show two broad peaks. These have been labeled d_1 and d_2 peaks by Cardona and Greenway (CG).²⁸ The centers of the d_1 peaks fall at 10.6, 10.1, and 9.7 eV, while the centers of the d_2 peaks fall at 14.6, 13.8, and 11.3 eV, respectively. Let us label valence or conduction p states by np (e.g., $n=4$ in Ge), core d states by $(n-1)d$, and conduction d states like $\Gamma_{12'}$ by nd . As noted by CG, the d_2 peaks look very similar to the $(n-1)d \rightarrow np$ peak observed³⁰ in 3-5 zincblende crystals between 19 and 23 eV. These were assigned to $(n-1)d$ levels on the trivalent ion. In the free atoms Zn and Cd the $(n-1)d \rightarrow p$ transition requires 11 or 12 eV. Thus, the assignment of the d_2 peak to these transitions is quite plausible.

There remain the d_1 peaks, which CG assume are due either to crystal-field splitting of the $(n-1)d$ levels on the divalent atoms, or to $(n-1)d \rightarrow$ higher p state in the conduction band. We find this assignment unconvincing for several reasons. The shape of the d_1 peak is quite different from the d_2 peak. The d_1-d_2 splitting changes substantially on going from Zn to Cd to Hg. Altogether it appears much more plausible to assign the d_1 structure to the M_1 and M_2 singularities seen in GaP, where the d_2 peak is centered at 23 eV. Thus, the

³⁰ H. R. Philipp and H. Ehrenreich, Phys. Rev. Letters 8, 92 (1962).

$L_3' \rightarrow L_2'$ peak seen at about 10 eV in GaP appears at about 10 eV in ZnTe, CdTe, and HgTe as well.

3. WURTZITE BANDS AND SPECTRA

Many crystals (including ZnS itself) are found in both the cubic zincblende and the hexagonal wurtzite structures. The c/a ratio is usually within 1% of the ideal value 1.63. In such cases the arrangement of second as well as first neighbors is nearly the same in the two structures. For these reasons one expects the electronic properties of the two structures to be nearly the same if the tight-binding approximation is valid. Studies of the direct absorption edges (which correspond to $\Gamma_{25'} \rightarrow \Gamma_2'$ in Ge) apparently confirm this view. The example we will discuss most thoroughly is CdSe. Here the first ("infrared" in our nomenclature) absorption edge³¹ for $\mathbf{E} \parallel c$ is only 0.03 eV higher than that for $\mathbf{E} \perp c$. This apparently indicates²⁴ that the hexagonal modification of the electronic structure is too slight to be significant for the uv spectrum.

To make this idea precise we must include the spin-orbit splitting³¹ of the $\Gamma_5(p_x, p_y)$ level into states Γ_7 and Γ_9 separated by 0.43 eV. The center of gravity of the spin-orbit split levels Γ_9 and Γ_7 is then 0.2 eV below that of the $\Gamma_1(p_z, \Gamma_7)$ of the double group).

A more convincing macroscopic argument for the absence of polarization effects is based on the low-frequency dielectric constant, which is given by

$$\epsilon_1(0) = 1 + \frac{1}{\pi} \int_{-\infty}^{\infty} \epsilon_2(\omega) \frac{d\omega}{\omega}. \quad (3.1)$$

The measured values of $\epsilon_1(0)$ for \mathbf{E} parallel or perpendicular to the c axis differ in³² CdS by about $\frac{1}{2}\%$. Nevertheless, as an earlier version of this paper predicted, polarization splittings of order 1 eV have been found.²⁵ This shows the unreliability of both tight-binding and macroscopic pictures of the electronic structure.

To carry out the idea that uv structure is primarily determined by the Brillouin zone, one must attempt to fit the hexagonally prismatic Brillouin zone of wurtzite into the truncated octahedral Brillouin zone of the zincblende structure. For this purpose it is convenient to use the double-zone scheme for the wurtzite zone. According to Birman,³³ a natural fit is obtained by identifying the c axis $\Gamma A \Gamma$ in wurtzite with a $[111]$ axis $\Gamma A \Gamma$ in the zincblende structure. The two Brillouin zones then fit together as shown in Fig. 9. This correspondence can be used³³ to describe stacking faults.

To interpret the uv spectrum (see Fig. 10) we need the energy levels $E(\mathbf{k})$ (see Fig. 11). Partly because of a paucity of experimental information and partly because of the

³¹ T. O. Dimmock and R. G. Wheeler, Phys. Rev. 125, 1803 (1962).

³² S. J. Czyzak, W. M. Baker, R. C. Crane, and J. B. Howe, J. Opt. Soc. Am. 47, 240 (1957).

³³ J. L. Birman, Phys. Rev. 115, 1493 (1959).

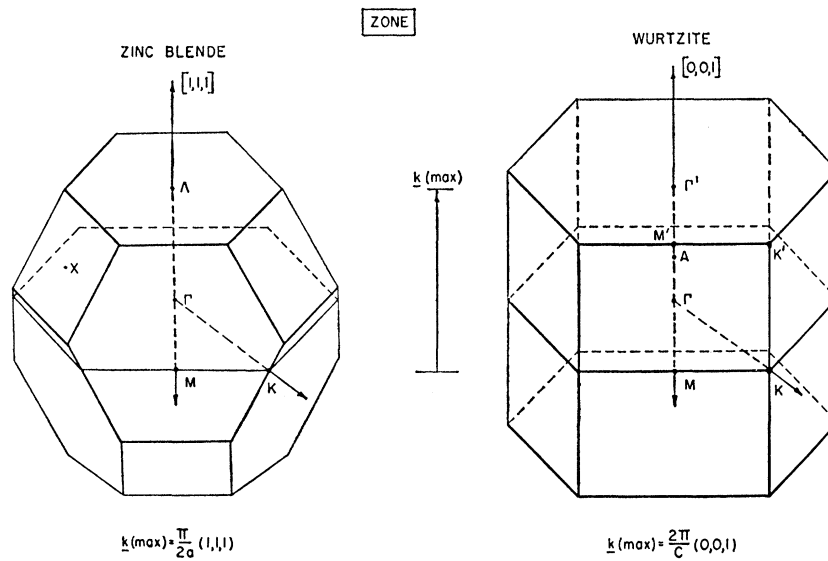


FIG. 9. Comparison of the Brillouin zones of the zincblende and wurtzite crystal structures (or fcc and hcp).

additional complexity of a structure of lower symmetry with four atoms per unit cell, no calculation seems to be available at present of sufficient accuracy. We do, however, anticipate a strong similarity between the wurtzite and zincblende structures, and very accurate rules²³ are available which can be used to predict the $E(\mathbf{k})$ curves for CdSe that would be found in a hypothetical (\equiv) zincblende modification. By combining these with those results of band calculations,¹² which we have found in I, are insensitive to the detailed crystal potential, a tentative interpretation of the spectrum can be made.

Consider first the levels at Γ . We use the notation of Glasser.^{34,35} Because of the hexagonal symmetry the levels (Γ_5, Γ_1) show a small crystal splitting; they are derived from $\Gamma_{25'}$ of the diamond structure. On the other hand, ($\Gamma_6, \Gamma_3, \Gamma_3$) in the valence band are derived from (L_3', L_2', L_1) and show a large crystal-field splitting. Data on diamond and zincblende crystals show that the energy difference ($\Gamma_{25'}, L_3'$) is rather insensitive to changes

in crystal potential or atomic composition.⁹ We therefore put $\Gamma_{5v} - \Gamma_{6v}$ in the valence band equal to 1.4 eV, the value appropriate to Ge.¹⁷

The positions of the conduction band levels Γ_{6c} and Γ_{5c} can be estimated in several ways. One can estimate $\Gamma_{5c} - \Gamma_{5v}$ from the extrapolated energy difference $\Gamma_{15} - \Gamma_{25'}$ of the equivalent diamond structure.²⁴ For CdSe this gives 6.5 eV. This difference should be insensitive to details of the crystal potential and can therefore be taken from Herman's calculations¹² for ZnS. This gives 7.5 eV. Both values are suggestively close to an edge in CdSe at 6.3 eV.

To locate Γ_{6c} one may extrapolate²⁸ (L_3, L_3) to estimate $\Gamma_{6c} - \Gamma_{6v}$. This gives 10.5 eV. Or one may take Herman's calculated value for $\Gamma_{6c} - \Gamma_{5c} \approx \Gamma_{5v} - \Gamma_{6v} \approx 1.4$ eV. Together with $\Gamma_{5c} - \Gamma_{5v}$ this gives $\Gamma_{6c} - \Gamma_{6v} = 9.1$ eV. Both estimates agree fairly well with the peaks in CdS, CdSe, and ZnS, labeled E_1' by Cardona,²⁴ which occur near 9.5 eV.

The remaining allowed interband transition at $\Gamma, \Gamma_{6v} \rightarrow \Gamma_{3c}$, is probably too weak to be resolved. The results at Γ , together with the appropriate polarization selection rules, are collected in Table III.

We now consider the new data²⁵ taken with a conventional polarizer below 6 eV. (Note that with a LiF polarizer it should be possible to check the polarizations of the E_0' and E_1' peaks given in Table III.) Much more structure is resolved for $\mathbf{E} \perp c$ than for $\mathbf{E} \parallel c$. In particular in CdSe a spin-orbit doublet ($A_1 A_2$) is resolved. The splitting is $\Delta_{s-0} = 0.27$ eV. This is just $\frac{2}{3}$ of the splitting of the valence band at $\mathbf{k} = 0$, which shows that we are dealing with a (p_x, p_y) doublet. There is reason to believe³⁶ that spin-orbit splittings in the conduction band are smaller than in the valence band. Also, the ($A_1 A_2$) line shape is similar to that of the ($\Delta_3 A_1$) edge in Ge. We therefore identify these peaks with transitions from a

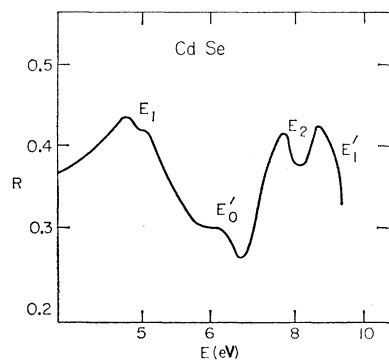


FIG. 10. The reflectance spectrum of hexagonal CdSe (unpolarized light).

³⁴ M. H. Cohen and L. M. Falicov, Phys. Rev. Letters 5, 544 (1960).

³⁵ Glasser interchanges Γ_5 and Γ_6 compared to the usual notation (e.g., Ref. 31). We adopt the convention that the top of the valence band is Γ_5 which transforms as (x, y) . We are grateful to Dr. Cardona for bringing this point to our attention.

³⁶ L. Liu and J. C. Phillips, Phys. Rev. Letters 8, 94 (1962).

doublet valence band edge to a singlet conduction band edge.

Doublet states are found on the line $\Delta=\Gamma A$, except near Γ and A , and along $P=KH$. On the basis of Herman's calculations¹² $K_3 \rightarrow K_2$ appears to be the most probable symmetry candidate for the (A_1A_2) doublet. At H , Herman's calculations suggest that the smallest band gap is (H_3, H_3) , which has parallel polarization. Thresholds of the M_0 type are present in the parallel polarization reflectance near 4.30 and 4.55 eV. These may be associated with $H_{3v} \rightarrow H_{3c}$ transitions, if we neglect the spin-orbit splitting of H_{3c} , as seems to be correct³⁶ for L_{3c} in Ge.

We now consider the large peaks $B = (4.86 \text{ eV}, \mathbf{E} \perp c)$ and $(B_1, B_2) = (4.77, 5.02 \text{ eV}, \mathbf{E} \parallel c)$. The line shapes of these peaks are qualitatively similar, and they occur at nearly the same energy. Nevertheless, the critical points responsible for the Van Hove singularities evidently occur in different bands, and there must be at least two of them in each polarization to produce such well-defined peaks, similar to the $X_4 \rightarrow X_1, \Sigma_4 \rightarrow \Sigma_1$ peaks in Si and Ge. Finally, although the separation of B_1 and B_2 is about the spin-orbit splitting, they occur for parallel polarization and have a line shape different from that of normal spin-orbit split peaks like (A_1A_2) . We conclude that there is no evidence for spin-orbit fine structure in these peaks, which therefore are not associated with the symmetry lines Δ or P .

The only remaining symmetry candidates are at M . (Transitions at L are excluded because the twofold orbital degeneracy there gives nonzero slopes.³⁷) To appreciate the complexity of the energy levels at M it is sufficient to note that each reciprocal lattice vector appears³⁴ in all symmetrized combinations of plane

TABLE III. Suggested assignments of interband transitions in CdSe. Most of the assignments at Γ agree with those of Ref. 24, but special emphasis is laid on the polarization of the edges in question. The polarization assignments below 6 eV agree with the data of Ref. 25. Above 6 eV the polarizations are unmeasured at present.

Transition	Polarization	Energy (eV)	Label
$\Gamma_5 \rightarrow \Gamma_1$	\perp	2.0	E_0
$\Gamma_1 \rightarrow \Gamma_1$	\parallel	1.8	E_0
$\Gamma_6 \rightarrow \Gamma_3$	\perp
$\Gamma_6 \rightarrow \Gamma_6$	\parallel	6.3	E_0'
$\Gamma_6 \rightarrow \Gamma_6$	\parallel	9.0	E_1'
$K_3 \rightarrow K_2$	\perp	4.18, 4.46	A_1A_2
$H_3 \rightarrow H_3$	\parallel	4.30, 4.55	
$M_4 \rightarrow M_3$	\perp	5.0?	B
$M_3 \rightarrow M_1$	\perp	5.0?	B
$M_1 \rightarrow M_1$	\parallel	5.0?	B_1B_2
$K_2 \rightarrow K_2$	\parallel	5.0?	B_1B_2

³⁷ L. M. Falicov and M. H. Cohen, Phys. Rev. **130**, 92 (1963).

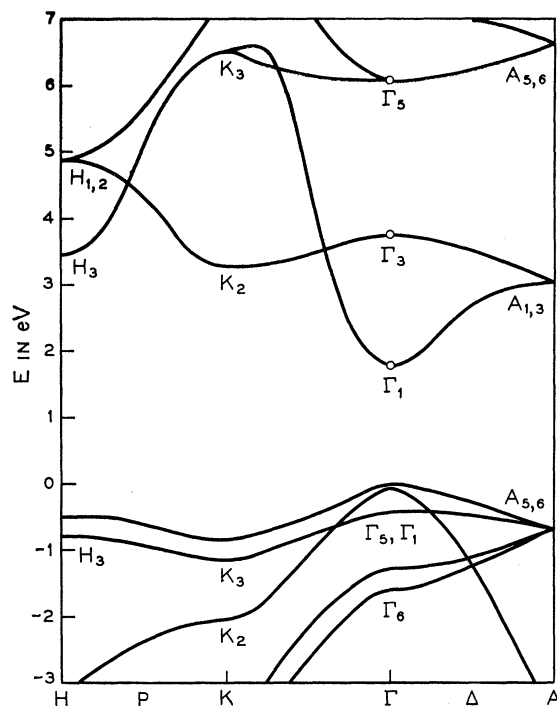


FIG. 11. A sketch of the energy bands of CdSe constructed to agree roughly with band calculations and in some details with the reflectance spectrum of Fig. 10 and the polarized spectrum of Ref. 25.

waves at M . Herman's results¹² show that this causes the states near the top of the valence band to be quite numerous. This is just the situation required to explain the peaks B and (B_1B_2) .

To be specific, the two singularities responsible for B could be due to $M_4 \rightarrow M_3$ and $M_3 \rightarrow M_1$. Band calculations¹² give about 5 eV for both transitions, which agrees better with experiment than one would have expected.

It is clearly difficult to find enough transitions for $\mathbf{E} \parallel c$ to explain all the (B_1B_2) structure. Possible candidates are $M_1 \rightarrow M_1$ and $K_2 \rightarrow K_2$.

ACKNOWLEDGMENTS

This paper was stimulated and influenced substantially in content by preprints and very relevant correspondence from Dr. M. Cardona. The author wishes to express his gratitude to Dr. Cardona for that assistance and at the same time absolve him of any responsibility for whatever errors have been made here. This manuscript was prepared in part while the author was visiting the Cavendish Laboratory and Bell Laboratories. It is a pleasure to thank the staff of both laboratories for their hospitality.